

# Heterosupramolecular Chemistry: Self-Assembly of an Electron Donor (TiO<sub>2</sub> Nanocrystallite)–Acceptor (Viologen) Complex<sup>†</sup>

Lucy Cusack, Xavier Marguerettaz, S. Nagaraja Rao, John Wenger, and Donald Fitzmaurice\*

Department of Chemistry, University College Dublin, Belfield, Dublin 4, Ireland

Received October 1, 1996. Revised Manuscript Received April 15, 1997<sup>®</sup>

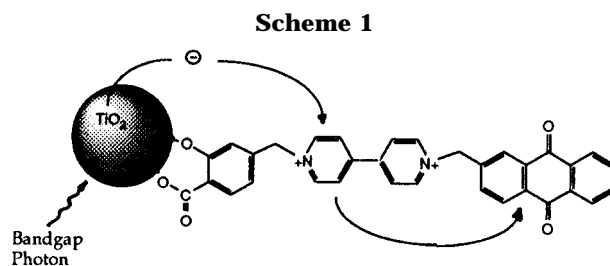
A TiO<sub>2</sub> nanocrystallite has been modified to selectively bind, by complementary hydrogen bonding, a uracil substrate incorporating a viologen moiety. Bandgap excitation of the self-assembled donor (TiO<sub>2</sub> nanocrystallite)–acceptor (viologen) complex results in electron transfer. Some implications of these findings for the self-assembly of functional nanostructures containing both condensed phase and molecular components are considered.

## Introduction

A heterosupramolecule is formed by linking condensed phase and molecular components.<sup>1</sup> As is the case for a supermolecule, the intrinsic properties of these components largely persist and there exists an associated heterosupramolecular function.<sup>2</sup> For example, the heterosupramolecule represented ideally in Scheme 1 consists of TiO<sub>2</sub> nanocrystallite, viologen, and anthraquinone components linked by surface coordination and formation of covalent bonds.<sup>3</sup> The associated heterosupramolecular function, light-induced vectorial electron transfer, has been demonstrated.<sup>4</sup> Also demonstrated, has been potentiostatic modulation of this function.<sup>5</sup>

As stated, the condensed phase and molecular components of the heterosupramolecule in Scheme 1 are linked by surface coordination and formation of covalent bonds. This is true of all heterosupramolecules prepared to date.<sup>1,3–5</sup> As a consequence self-processes, with the exception of self-organization, were precluded.<sup>6</sup> To address this limitation TiO<sub>2</sub> nanocrystallites stabilized by the modified pyridine **I** and denoted TiO<sub>2</sub>–**I** have been prepared.<sup>7</sup> These nanocrystallites selectively bind by complementary hydrogen bonding the modified uracil substrate **II** to form the complex represented ideally in Scheme 2 and denoted TiO<sub>2</sub>–(**I**+**II**).<sup>7</sup>

In a further development of these studies we report the self-assembly of the electron donor (TiO<sub>2</sub> nanocrystallite)–acceptor (viologen) complex represented ideally



in Scheme 2 and denoted TiO<sub>2</sub>–(**I**+**III**).<sup>8</sup> The associated function, light-induced vectorial electron transfer, is demonstrated. Some implications of these findings for the self-assembly of complex nanostructures containing both condensed phase and molecular components are considered.

## Results and Discussion

**I. Preparation and Characterization of a Model Supramolecular Complex.** Self-assembly, by complementary hydrogen bonding, of **I** and **II** in chloroform leads to formation of the supermolecule (**I**+**II**) represented ideally in Scheme 3. This complex, first prepared by Lehn and co-workers,<sup>9</sup> has recently been characterized in detail by <sup>1</sup>H NMR and FT-IR spectroscopies.<sup>7</sup> These studies allow us to determine whether **I** and **III** form an analogous supramolecular complex (**I**+**III**), represented ideally in Scheme 3, in the mixed solvent system chloroform-*d*/acetone-*d*<sub>6</sub> (1:1 by vol).

Shown in Figure 1 are the <sup>1</sup>H NMR spectra of (0.004 mol dm<sup>-3</sup>) **I**, **III**, and (**I**+**III**) in chloroform-*d*/acetone-*d*<sub>6</sub> (1:1 by vol). The singlet observed for **I** at δ 8.67 is assigned to the two equivalent amidic protons.<sup>10</sup> The singlets observed for **III** at δ 9.35 and 9.71 are assigned to the amidic and imidic protons of the uracil ring although,<sup>10</sup> in the absence of additional data it is not possible to uniquely assign these resonances.<sup>7</sup>

(8) Cusack, L.; Rao, S. N.; Fitzmaurice, D. *Angew. Chem., Int. Ed. Engl.* **1997**, *36*, 848.

(9) Brienne, M.-J.; Gabard, J.; Lehn, J.-M. *J. Chem. Soc., Chem. Commun.* **1989**, 1868.

(10) (a) Feibush, B.; Fiuroa, A.; Charles, R.; Onan, K.; Feibush, P.; Karger, B. *J. Am. Chem. Soc.* **1986**, *108*, 3310. (b) Feibush, B.; Saha, M.; Onan, K.; Karger, B.; Giese, R. *J. Am. Chem. Soc.* **1987**, *109*, 7531. (c) Hamilton, A.; Van Engen, D. *J. Am. Chem. Soc.* **1987**, *109*, 5035. (d) Bisson, A.; Carver, F.; Hunter, C.; Waltho, J. *J. Am. Chem. Soc.* **1994**, *116*, 10292.

<sup>†</sup> Dedicated to Prof. D. M. X. Donnelly on the occasion of her 65th birthday.

\* To whom correspondence should be addressed.

<sup>®</sup> Abstract published in *Advance ACS Abstracts*, June 1, 1997.

(1) Marguerettaz, X.; O'Neill, R.; Fitzmaurice, D. *J. Am. Chem. Soc.* **1994**, *116*, 2628.

(2) (a) Lehn, J.-M. *Supramolecular Chemistry*; VCH: New York, 1995. (b) Balzani, V.; Scandola, F. *Supramolecular Photochemistry*; Ellis Horwood: New York, 1991; Chapter 3.

(3) Marguerettaz, X.; Fitzmaurice, D. *J. Am. Chem. Soc.* **1994**, *116*, 5017.

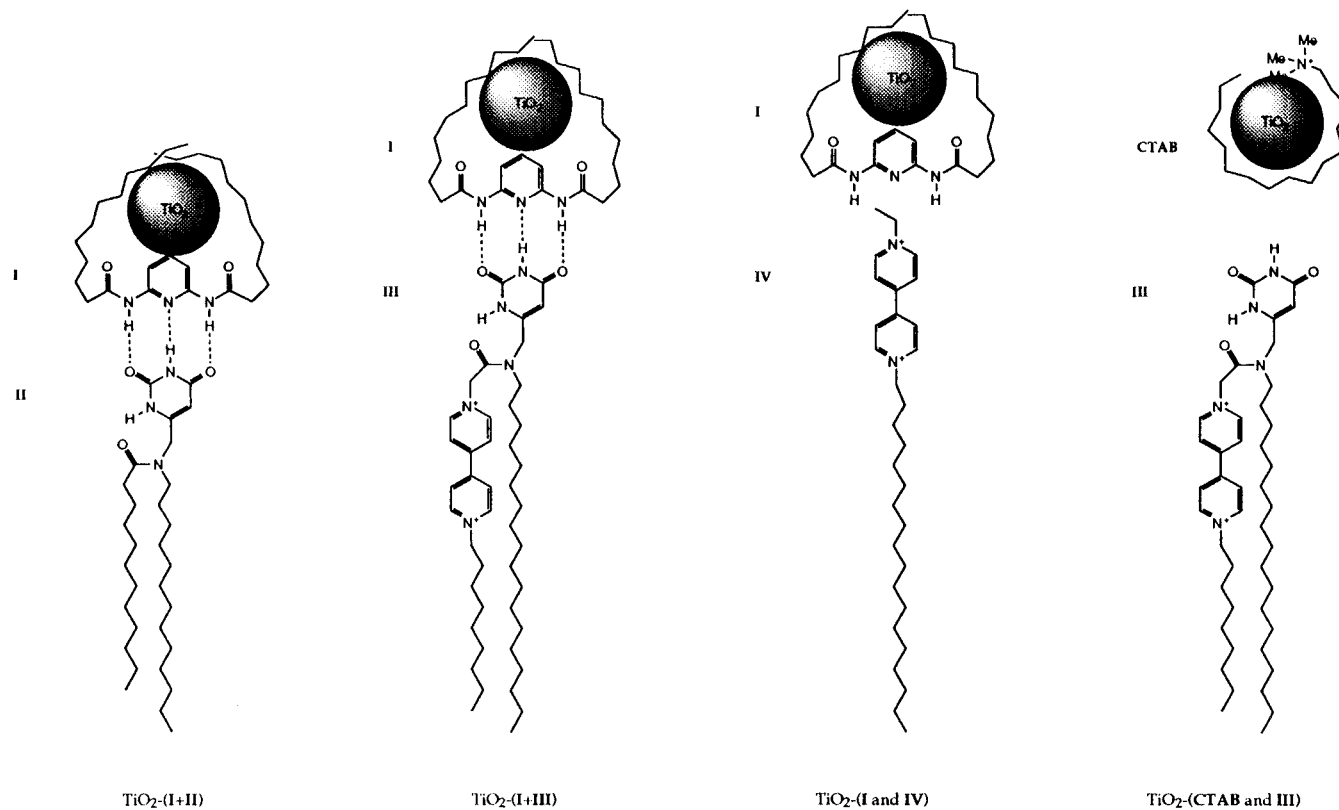
(4) Marguerettaz, X.; Redmond, G.; Rao, S. N.; Fitzmaurice, D. *SPIE Proc. Ser.* **1994**, *2255*, 793.

(5) Marguerettaz, X.; Redmond, G.; Rao, S. N.; Fitzmaurice, D. *Chem. Eur. J.* **1996**, *2*, 420.

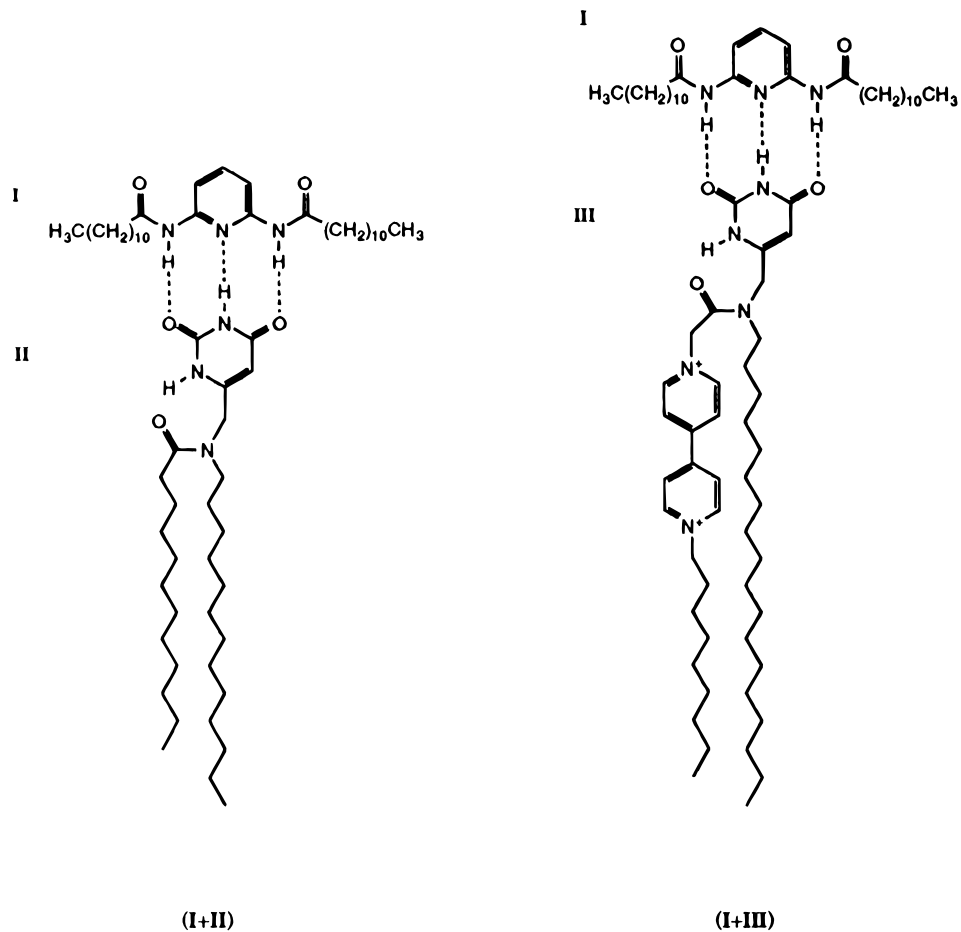
(6) (a) Philp, D.; Stoddart, J. F. *Synlett* **1991**, 445. (b) Lindsey, J. S. *New J. Chem.* **1991**, *15*, 153. (c) Whitesides, G. M.; Mathias, J. P.; Seto, C. T. *Science* **1991**, *254*, 1312.

(7) Cusack, L.; Rao, S. N.; Wenger, J.; Fitzmaurice, D. *Chem. Mater.* **1997**, *9*, 624.

Scheme 2



Scheme 3



For **(I+III)**, proton resonances are observed at  $\delta$  8.76, 9.42, and 9.91. The resonance at  $\delta$  8.76 for **(I+III)**

clearly correlates, based on a comparison of integrated peak areas, with that of the amidic protons at  $\delta$  8.67 in

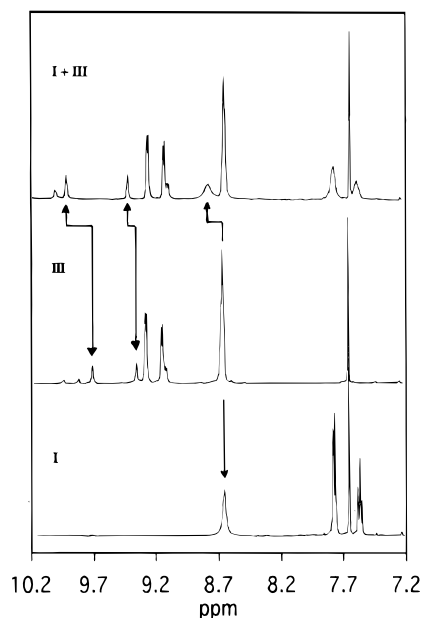


**Figure 1.**  $^1\text{H}$  NMR spectra of  $0.004 \text{ mol dm}^{-3}$  of **I**, **III**, and **(I+III)** in chloroform-*d*/acetone-*d*<sub>6</sub> (1:1 by vol) at  $20^\circ\text{C}$ .

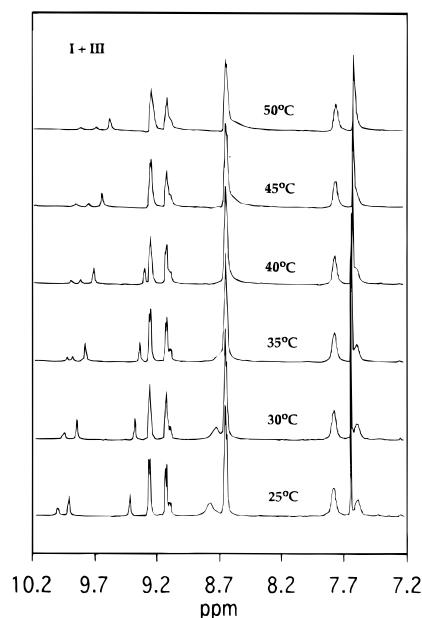


**Figure 2.**  $^1\text{H}$  NMR spectra of  $0.004 \text{ mol dm}^{-3}$  of **(I+III)** in chloroform-*d*/acetone-*d*<sub>6</sub> (1:1 by vol) at the indicated temperatures.

**I.** To correlate the resonances at  $\delta$  9.42 and 9.91 in **(I+III)** with the corresponding resonances in **III**, temperature-dependent  $^1\text{H}$  NMR studies were undertaken; see Figure 2. As expected, the two proton resonance at  $\delta$  8.76 for **(I+III)** shifts upfield to  $\delta$  8.67 upon raising the sample temperature to  $50^\circ\text{C}$ . The one-proton resonance at  $\delta$  9.42 in **(I+III)** shows a significantly weaker temperature dependence up to  $50^\circ\text{C}$  and correlates with the singlet at  $\delta$  9.35 for **III**. The one-proton resonance at  $\delta$  9.91 for **(I+III)** shifts upfield upon raising the sample temperature to  $50^\circ\text{C}$  and correlates with the resonance at  $\delta$  9.71 for **III**. In short, the proton resonances at  $\delta$  8.67 in **I** and  $\delta$  9.35 and 9.71 in **III** correlate with those observed at  $\delta$  8.76, 9.41, and 9.91 in **(I+III)**, respectively.

The above findings require assignment of the resonances at  $\delta$  8.76 and 9.91 in **(I+III)** to intermolecularly

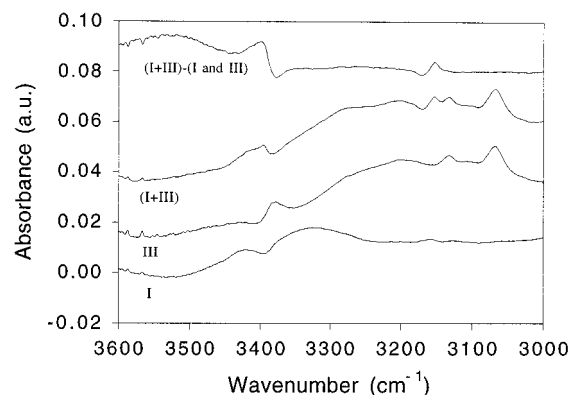


**Figure 3.** FT-IR spectra of  $0.004 \text{ mol dm}^{-3}$  of **I**, **III**, and **(I+III)** in chloroform-*d*/acetone-*d*<sub>6</sub> (1:1 by vol) at  $20^\circ\text{C}$ .

hydrogen-bonded protons for the following reasons: first, both resonances shift downfield upon formation of **(I+III)**; second, both resonances shift upfield to values close to those observed for the free components **I** and **III** upon raising the sample temperature to  $50^\circ\text{C}$ .<sup>10</sup> It is noted, that these downfield shifts are significantly smaller than those observed following formation of the supramolecular complex **(I+II)** in chloroform-*d*.<sup>7</sup> This observation is accounted for by the facts that the above resonances are previously shifted downfield and that the strength of the resulting intermolecular interaction is reduced due, in both cases, to the presence of acetone-*d*<sub>6</sub>. Concerning the proton resonance at  $\delta$  9.41 in **(I+III)**, its position is not shifted downfield significantly in the presence of acetone-*d*<sub>6</sub> as a solvent component.<sup>7</sup> Neither, is this resonance shifted downfield significantly upon formation of **(I+III)**. Further, the position of this resonance is only weakly temperature dependent. On this basis, we conclude that this proton does not form an intermolecular hydrogen bond in **(I+III)** but, as is the case in **(I+II)**, forms an intramolecular hydrogen bond in **III**.<sup>7</sup> Further support for this assertion is provided by the corresponding FT-IR studies reported below. On the basis of the above findings the resonances at  $\delta$  9.35 and 9.71 in **III** and  $\delta$  9.41 and 9.91 in **(I+III)** are assigned to the amidic and imidic protons of the uracil ring, respectively.

Shown in Figure 3 are the FT-IR spectra of ( $0.004 \text{ mol dm}^{-3}$ ) **I**, **III**, and **(I+III)** in chloroform-*d*/acetone-*d*<sub>6</sub> (1:1 by vol). The band previously observed for **I** at  $3423 \text{ cm}^{-1}$  in chloroform-*d*<sup>7</sup> and assigned to the  $-\text{NH}$  stretch of the amidic protons is broadened and reduced in intensity.<sup>7,11–14</sup> Further, it is possible that an additional weak and broad feature is observed at  $3330 \text{ cm}^{-1}$  that would be assigned to the amidic protons of **I** hydrogen bonded to the acetone component of the mixed solvent system. The band previously observed for **II** at  $3395 \text{ cm}^{-1}$  in chloroform-*d*<sup>7</sup> and assigned to the  $-\text{NH}$  stretch of the imidic proton of the uracil ring is also broadened

(11) Bellamy, L. J. *The Infrared Spectra of Complex Molecules*; Mathuen: London, 1954.

(12) (a) Tsuboi, M. *Appl. Spectrosc. Rev.* **1969**, *3*, 45. (b) Susi, H.; Ard, J. *Spectrochim. Acta* **1971**, *27A*, 1549.

(13) (a) Hamlin, R.; Lord, R.; Rich, A. *Science* **1965**, *148*, 1734. (b) Kyogoku, Y.; Lord, R.; Rich, A. *Proc. Natl. Acad. Sci. U.S.A.* **1967**, *57*, 250. (c) Kyogoku, Y.; Lord, R.; Rich, A. *J. Am. Chem. Soc.* **1967**, *89*, 496. (d) Kyogoku, Y.; Lord, R.; Rich, A. *Biochim. Biophys. Acta* **1969**, *179*, 10. (e) Zundel, G.; Lubos, W.; Kolkenbeck, K. *Can. J. Chem.* **1971**, *49*, 3795.

(14) Pimentel, G.; McClellan, A. *The Hydrogen Bond*; Freeman: San Francisco, 1956.

and reduced in intensity.<sup>7,11–14</sup> Further, an additional broad feature is observed at 3200 cm<sup>-1</sup> that is assigned to the amidic and imidic protons of **III** hydrogen bonded to the acetone component of the mixed solvent system.<sup>11–14</sup> As a consequence, the spectral changes that accompany the mixing of equimolar quantities of **I** and **III** in chloroform-*d*/acetone-*d*<sub>6</sub> are less pronounced than those previously observed upon mixing of equimolar quantities of **I** and **II** in chloroform-*d*.<sup>7</sup> However, as would be expected the bands at 3423 and 3395 cm<sup>-1</sup> assigned to the amidic and imidic protons of **I** and **III**, respectively, are further reduced in intensity while it is possible that a new weak broad feature is observed at 3300 cm<sup>-1</sup> that is assigned to the intermolecular hydrogen bonds in (**I+III**). These changes are apparent in the difference spectrum (**I+III**) + (**I** and **III**).

In short, both the <sup>1</sup>H NMR and FT-IR studies described above support the view that **I** and **III** form the supramolecular complex (**I+III**) represented ideally in Scheme 3 by complementary hydrogen bonding in a chloroform-*d*/acetone-*d*<sub>6</sub> mixed solvent system (1:1 by vol).

**II. Preparation and Characterization of a Heterosupramolecular Donor–Acceptor Complex.** TiO<sub>2</sub> nanocrystallites were prepared in chloroform-*d* by arrested hydrolysis of titanium tetraisopropoxide in the presence of added (0.004 mol dm<sup>-3</sup>) **I** as a stabilizer.<sup>15</sup> The nanocrystallite (particle) concentration was calculated to be 4 × 10<sup>-7</sup> mol dm<sup>-3</sup>.<sup>16</sup> The resulting sol, denoted TiO<sub>2</sub>-**I**, was characterized by UV–vis absorption spectroscopy and by transmission electron microscopy. The absorption onset and average crystallite diameter of 360 nm and 22 ± 2 Å, respectively, are in good agreement with reported values.<sup>15,17</sup>

An important issue, addressed in detail elsewhere,<sup>7</sup> is the extent to which **I** interacts with the surface of a TiO<sub>2</sub> nanocrystallite in TiO<sub>2</sub>-**I**. Briefly, the above sol is as stable as those prepared using conventional stabilizers, indicating that some fraction of **I** is at the surface of the dispersed nanocrystallites. Consistent with this assertion is the observation that in the absence of added **I** the resulting sol is highly scattering and unstable over a period of minutes. More quantitatively, high-resolution <sup>1</sup>H NMR spectra of **I** and TiO<sub>2</sub>-**I** have been measured. An additional resonance is observed in the range δ 0.8–δ 0.9 for TiO<sub>2</sub>-**I**.<sup>7</sup> This resonance is assigned to the terminal methyl groups of the alkane side chains of **I** at the surface of a TiO<sub>2</sub> nanocrystallite. From an analysis of these spectra it is estimated that about 50% of **I** are at the surface of a TiO<sub>2</sub> nanocrystallite in TiO<sub>2</sub>-**I**. It should be noted that as the concentration of added stabilizer is reduced, a greater fraction of these molecules are adsorbed at the nanocrystallite surface. A systematic study of these and related compounds adsorbed at the surface of dispersed nanocrystallites is in progress.<sup>18</sup>

It was expected, based on the findings presented in section I, that addition of **III** in acetone-*d* to TiO<sub>2</sub>-**I** in

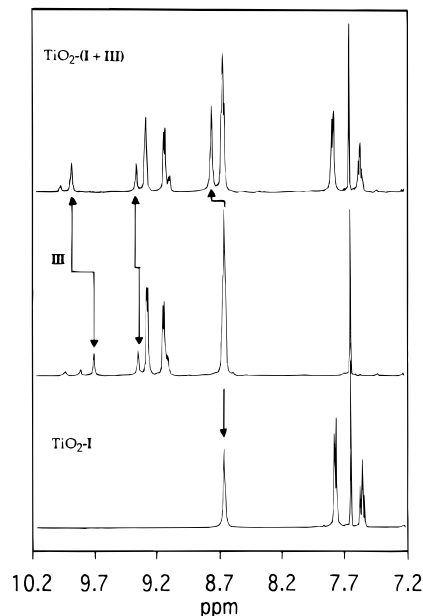


**Figure 4.** <sup>1</sup>H NMR spectra of 0.004 mol dm<sup>-3</sup> of TiO<sub>2</sub>-**I**, **III**, and TiO<sub>2</sub>-(**I+III**) in chloroform-*d*/acetone-*d*<sub>6</sub> (1:1 by vol) at 20 °C. The concentration of TiO<sub>2</sub> nanocrystallites is 4 × 10<sup>-7</sup> mol dm<sup>-3</sup>.

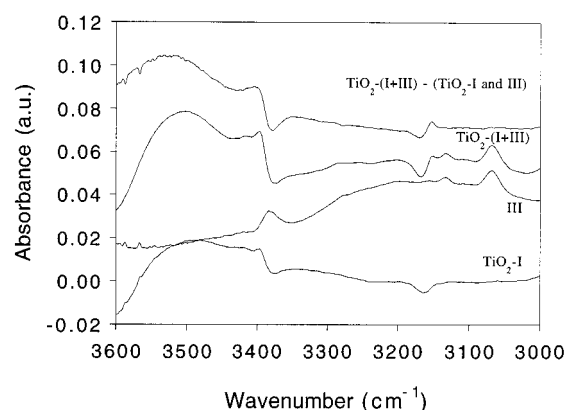


**Figure 5.** FT-IR spectra of 0.004 mol dm<sup>-3</sup> of TiO<sub>2</sub>-**I**, **III**, and TiO<sub>2</sub>-(**I+III**) in chloroform-*d*/acetone-*d*<sub>6</sub> (1:1 by vol) at 20 °C. The concentration of TiO<sub>2</sub> nanocrystallites is 4 × 10<sup>-7</sup> mol dm<sup>-3</sup>.

chloroform-*d* would result in self-assembly of the heterosupramolecular donor–acceptor complex TiO<sub>2</sub>-(**I+III**) represented ideally in Scheme 2. To test this expectation, detailed <sup>1</sup>H NMR and FT-IR studies were undertaken.

Shown in Figure 4 are the <sup>1</sup>H NMR spectra of (0.004 mol dm<sup>-3</sup>) TiO<sub>2</sub>-**I**, **III**, and TiO<sub>2</sub>-(**I+III**) in chloroform-*d*/acetone-*d*<sub>6</sub> (1:1 by vol). These spectra are in excellent agreement with those of **I**, **III**, and (**I+III**) shown in Figure 1. Specifically, the amidic proton resonances of TiO<sub>2</sub>-**I** are observed at δ 8.67. The amidic and imidic proton resonances of **III** are observed at δ 9.35 and 9.70, respectively. For TiO<sub>2</sub>-(**I+III**) the above resonances are observed at δ 8.76, 9.36, and 9.88, respectively.

Shown in Figure 5 are the FT-IR spectra of (0.004 mol dm<sup>-3</sup>) TiO<sub>2</sub>-**I**, **III**, and TiO<sub>2</sub>-(**I+III**) in chloroform-*d*/acetone-*d*<sub>6</sub> (1:1 by vol). These spectra are in good agreement with those of **I**, **III**, and (**I+III**) shown in Figure 3. (The additional band observed for samples containing TiO<sub>2</sub> nanocrystallites at about 3500 cm<sup>-1</sup> is assigned to surface hydroxyl groups.) As in Figure 3,

(15) Kotov, N.; Meldrum, F.; Fendler, J. *J. Phys. Chem.* **1994**, *98*, 8827.

(16) This calculation assumed complete conversion of the precursors and that the average crystallite diameter was 22 ± 2 Å.

(17) Serpone, N.; Lawless, D.; Khairutdinov, R. *J. Phys. Chem.* **1995**, *99*, 16646.

(18) Rizza, R.; Merrins, A.; Fitzmaurice, D., manuscript in preparation.

the absorption band at  $3423\text{ cm}^{-1}$  in  $\text{TiO}_2\text{-I}$  and  $3395\text{ cm}^{-1}$  in **III** are reduced in intensity in  $\text{TiO}_2\text{-(I+III)}$ , while it is possible that a weak broad feature is observed at about  $3300\text{ cm}^{-1}$ . These changes are apparent in the difference spectrum  $\text{TiO}_2\text{-(I+III)} + (\text{TiO}_2\text{-I and III})$ .

In short, both the  $^1\text{H NMR}$  and FT-IR studies described above support the view that  $\text{TiO}_2\text{-I}$  and **III** form, by complementary hydrogen bonding, the supramolecular complex  $\text{TiO}_2\text{-(I+III)}$  represented ideally in Scheme 2 in a chloroform-*d*/acetone-*d*<sub>6</sub> mixed solvent system (1:1 by vol).

To further increase confidence in the above assignments,  $^1\text{H NMR}$  spectra (not shown) were recorded for ( $0.004\text{ mol dm}^{-3}$ )  $\text{TiO}_2\text{-CTAB}$ , **III**, and  $\text{TiO}_2\text{-(CTAB and III)}$  in chloroform-*d*/acetone-*d*<sub>6</sub> (1:1 by vol). There is no evidence for selective binding of **III** by  $\text{TiO}_2\text{-CTAB}$  to form a complex similar to  $\text{TiO}_2\text{-(I+III)}$ , i.e., no downfield shift is observed for the imidic proton resonance of **III**. Thus in the absence of a stabilizer that contains the diaminopyridine moiety, a  $\text{TiO}_2$  nanocrystallite will not recognize or selectively bind the modified substrate **III**.

$^1\text{H NMR}$  spectra (not shown) were also recorded for ( $0.004\text{ mol dm}^{-3}$ )  $\text{TiO}_2\text{-I}$ , **IV**, and  $\text{TiO}_2\text{-(I and IV)}$  in chloroform-*d*/acetone-*d*<sub>6</sub> (1:1 by vol). Again, there is no evidence for selective binding of **IV** by  $\text{TiO}_2\text{-I}$  to form a complex similar to  $\text{TiO}_2\text{-(I+III)}$ , i.e., no downfield shift is observed for the amidic proton resonance of **I** in  $\text{TiO}_2\text{-I}$ . Thus the modified nanocrystallite  $\text{TiO}_2\text{-I}$  will not recognize or selectively bind a substrate the uracil moiety.

**III. Demonstration of Light-Induced Electron Transfer in a Heterosupramolecular Donor-Acceptor Complex.** On the basis of the above findings it was expected that bandgap excitation of a  $\text{TiO}_2$  nanocrystallite in  $\text{TiO}_2\text{-(I+III)}$  would result in immediate electron transfer from  $\text{TiO}_2\text{-I}$  to the viologen moiety of hydrogen-bonded **III**. However, it was expected that bandgap excitation would also result in electron transfer from  $\text{TiO}_2\text{-I}$  to the viologen moiety of diffusionally encountered **III**. In the cases of either  $\text{TiO}_2\text{-(I and IV)}$  or  $\text{TiO}_2\text{-(CTAB and III)}$  it was expected that bandgap excitation would result only in electron transfer from either  $\text{TiO}_2\text{-I}$  or  $\text{TiO}_2\text{-CTAB}$  to the viologen moiety of diffusionally encountered **IV** or **III**, respectively.

It is noted that the molecular component concentration was  $4 \times 10^{-4}\text{ mol dm}^{-3}$  for all transient absorption experiments reported and, that under these conditions, about 70% of **I** or CTAB are at the nanocrystallite surface.<sup>7</sup> The nanocrystallite (particle) concentration was, as above, calculated to be  $4 \times 10^{-7}\text{ mol dm}^{-3}$ .<sup>16</sup> Finally, we note that all transient absorption measurements were performed in nondeuterated solvents.

Shown in Figure 6, are micro- and millisecond absorption transients and steady-state absorption spectra measured following bandgap excitation of  $\text{TiO}_2\text{-I}$  in chloroform/acetone (1:1 by vol). Concerning the above we note the following: First, the microsecond transient is not measurably dependent on the extent to which  $\text{TiO}_2\text{-I}$  is degassed. Second, while the millisecond transient for degassed  $\text{TiO}_2\text{-I}$  decays to about 50% of its initial amplitude between pulses, the same transient for aerated  $\text{TiO}_2\text{-I}$  decays fully. Third, while the visible spectrum measured following bandgap irradiation of degassed  $\text{TiO}_2\text{-I}$  agrees with that reported for photo-

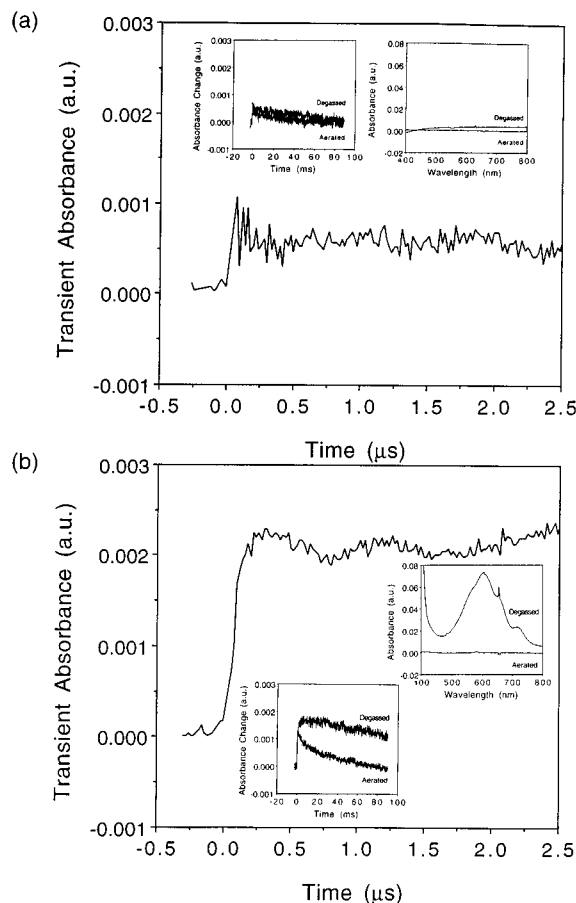


**Figure 6.** (a) Transient absorption at 600 nm for degassed  $\text{TiO}_2\text{-I}$  in a chloroform/acetone mixture (1:1: by vol) at  $20^\circ\text{C}$  on the microsecond time scale following bandgap excitation at 355 nm (average of 10 pulses of 5 ns duration at 2 mJ per pulse). Also shown are the absorption transients for degassed and aerated  $\text{TiO}_2\text{-I}$  in a chloroform/acetone mixture (1:1: by vol) at  $20^\circ\text{C}$  on the millisecond time scale (average of 100 pulses of 5 ns duration at 2 mJ/pulse) and the corresponding absorption spectra measured following irradiation. (b) As in (a) for  $\text{TiO}_2\text{-(I+III)}$ .

generated electrons trapped in a  $\text{TiO}_2$  nanocrystallite,<sup>19,20</sup> no spectrum is measured for aerated  $\text{TiO}_2\text{-I}$  under the same conditions. Fourth, on the basis of the final amplitude of the millisecond transient for degassed  $\text{TiO}_2\text{-I}$  (0.0001 au), an irradiation volume of  $0.4\text{ cm}^3$  (effective path length of 0.7 cm) and a sample volume of  $1.8\text{ cm}^3$  one predicts, in good agreement with the measured spectrum, a steady-state absorption of 0.003 au at 600 nm. On this basis, the microsecond transient in Figure 6a is assigned to long-lived electrons trapped in the  $\text{TiO}_2$  nanocrystallite of  $\text{TiO}_2\text{-I}$ . Finally, as there is no measurable absorption by the molecular component **I** at 355 nm, no transients are measured for **I**.

Also shown in Figure 6, are microsecond and millisecond absorption transients and steady-state absorption spectra measured following bandgap excitation of

(19) (a) Henglein, A. *Ber. Bunsen-Ges. Phys. Chem.* **1982**, *86*, 246. (b) Duonghong, D.; Ramsden, J.; Grätzel, M. *J. Am. Chem. Soc.* **1982**, *104*, 2977. (c) Kolle, U.; Moser, J.; Grätzel, M. *Inorg. Chem.* **1985**, *24*, 2253. (d) Rothenberger, G.; Moser, J.; Grätzel, M.; Serpone, N.; Sharma, D. *J. Am. Chem. Soc.* **1985**, *107*, 8054.

(20) There is general agreement that the spectrum of trapped holes does not extend to wavelengths longer than about 450 nm: (a) Bahnemann, D.; Henglein, A.; Lilie, J.; Spanhel, L. *J. Phys. Chem.* **1984**, *88*, 709. (b) Micic, O.; Zhang, Y.; Cromack, R.; Trifunac, A.; Thurnauer, M. *J. Phys. Chem.* **1993**, *97*, 7277.

TiO<sub>2</sub>-(**I+III**) in chloroform/acetone (1:1 by vol). Concerning the above we note the following: First, the microsecond transient is not measurably dependent on the extent to which TiO<sub>2</sub>-(**I+III**) is degassed. Second, while the millisecond transient for degassed TiO<sub>2</sub>-(**I+III**) rises initially within the laser pulse and slowly during 10 ms, the millisecond transient for aerated TiO<sub>2</sub>-(**I+III**) rises only within the laser pulse. Third, while the millisecond transient for degassed TiO<sub>2</sub>-(**I+III**) decays to about 80% of its initial amplitude, the same transient for aerated TiO<sub>2</sub>-(**I+III**) decays fully. Fourth, while the visible spectrum measured following bandgap irradiation of degassed TiO<sub>2</sub>-(**I+III**) agrees well with that reported for the radical cation of viologens<sup>21</sup> and as expected is offset from the baseline by about 0.003 au due to the presence of long-lived electrons trapped in the TiO<sub>2</sub> nanocrystallites of TiO<sub>2</sub>-**I**.<sup>19,20</sup> No spectrum is measured for aerated TiO<sub>2</sub>-(**I+III**) under the same conditions. Fifth, on the basis of the final amplitude (0.0015 au) of the millisecond transient for degassed TiO<sub>2</sub>-(**I+III**), an irradiation volume of 0.4 cm<sup>3</sup> and a sample volume of 1.4 cm<sup>3</sup> one predicts a steady-state absorption, in good agreement with the measured spectrum, of 0.06 au at 600 nm. On this basis, the microsecond transient in Figure 6b is assigned to the radical cation of **III** and to long-lived electrons trapped in the TiO<sub>2</sub> nanocrystallite of TiO<sub>2</sub>-(**I+III**). Also on this basis, the slow component of the millisecond transient for degassed TiO<sub>2</sub>-(**I+III**) is assigned to the radical cation of **III** formed by diffusion to TiO<sub>2</sub>-**I**.<sup>22</sup> It is noted that the contribution to the measured transient for degassed TiO<sub>2</sub>-(**I+III**) by trapped electrons may be accurately deduced from the transient measured for degassed TiO<sub>2</sub>-**I**. Finally, as there is no measurable absorption by the molecular components **I** or **III** at 355 nm, no transients are measured for **I**, **III**, or (**I+III**).

Shown in Figure 7 are microsecond and millisecond absorption transients and steady-state absorption spectra measured for TiO<sub>2</sub>-(**I** and **IV**) in chloroform/acetone (1:1 by vol). Concerning the above we note the following: First, the microsecond transient is not measurably dependent on the extent to which TiO<sub>2</sub>-(**I** and **IV**) is degassed. Second, while the millisecond transient for degassed TiO<sub>2</sub>-(**I** and **IV**) rises within the laser pulse and slowly during 10 ms, the millisecond transient for aerated TiO<sub>2</sub>-(**I** and **IV**) rises only within the laser pulse. Third, while the millisecond transient for degassed TiO<sub>2</sub>-(**I** and **IV**) decays to about half its maximum amplitude, the same transient for aerated TiO<sub>2</sub>-(**I** and **IV**) decays fully and agrees well with that for aerated TiO<sub>2</sub>-**I**. Fourth, while the visible spectrum measured following bandgap irradiation of degassed TiO<sub>2</sub>-(**I** and **IV**) agrees well with that reported for the radical cation of viologens<sup>21</sup> and is offset from the baseline by about 0.003 au due to the presence of long-lived electrons trapped in the TiO<sub>2</sub> nanocrystallites of TiO<sub>2</sub>-**I**.<sup>19,20</sup> No spectrum is measured for aerated TiO<sub>2</sub>-(**I** and **IV**) under the same conditions. Fifth, on the basis of the difference of the final amplitudes of the millisecond transients (0.0005 au), an irradiation volume of 0.4 cm<sup>3</sup>, and a sample volume of 1.4 cm<sup>3</sup> one predicts a steady-state absorption of 0.02 au at 600 nm

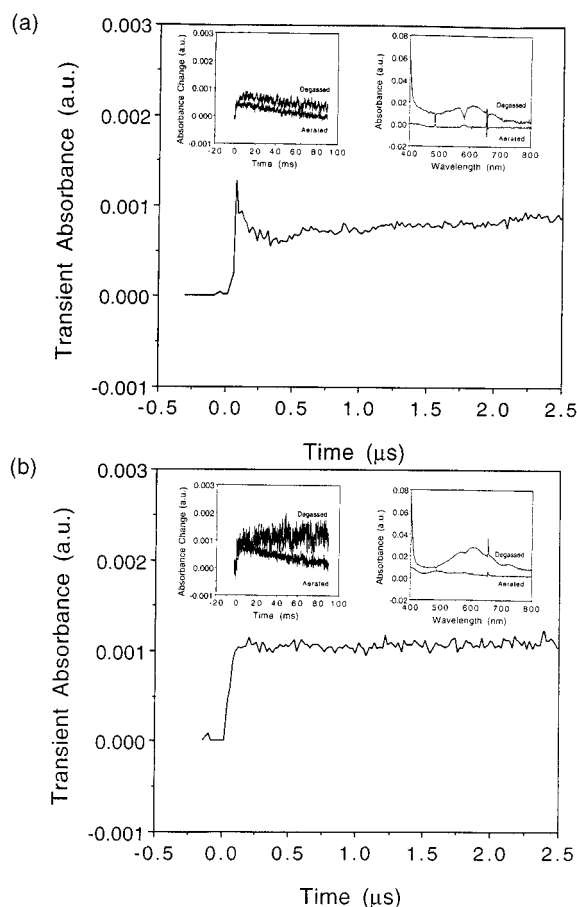


**Figure 7.** (a) Transient absorption at 600 nm for degassed TiO<sub>2</sub>-(**I** and **IV**) in a chloroform/acetone mixture (1:1: by vol) at 20 °C on the microsecond time scale following bandgap excitation at 355 nm (average of 10 pulses of 5 ns duration at 2 mJ/pulse). Also shown are the absorption transients for degassed and aerated TiO<sub>2</sub>-(**I** and **IV**) in a chloroform/acetone mixture (1:1: by vol) at 20 °C on the millisecond time scale (average of 100 pulses of 5 ns duration at 2 mJ/pulse) and the corresponding absorption spectra measured following irradiation. (b) As in (a) for TiO<sub>2</sub>-(**CTAB** and **III**).

for degassed TiO<sub>2</sub>-(**I** and **IV**) by reduced **IV**. On this basis, the microsecond transient in Figure 7a is assigned to electrons trapped in a TiO<sub>2</sub> nanocrystallite and to the radical cation of **IV** formed by diffusion to TiO<sub>2</sub>-**I**.<sup>22</sup> Finally, as there is no measurable absorption by the molecular components **I** or **IV** at 355 nm, no transients are measured for **I**, **IV**, or (**I** and **IV**).

Also shown in Figure 7 are the microsecond and millisecond absorption transients and steady-state absorption spectra measured for TiO<sub>2</sub>-(**CTAB** and **III**) in chloroform/acetone. Qualitatively, they agree with those measured for TiO<sub>2</sub>-(**I** and **IV**), although the following quantitative differences are noted: First, the millisecond transients for degassed and aerated TiO<sub>2</sub>-(**CTAB** and **III**) decay more slowly.<sup>23</sup> Therefore, while the visible spectrum measured following bandgap irradiation of degassed TiO<sub>2</sub>-(**CTAB** and **III**) agrees well with that reported for the radical cation of viologen,<sup>21</sup> it is offset from the baseline by about 0.006 au, twice the value for degassed TiO<sub>2</sub>-(**I** and **IV**), due to the

(21) (a) Kok, B.; Rurainski, H.; Owens, O. *Biochem. Biophys. Acta* **1965**, *109*, 347. (b) Trudinger, P. *Anat. Biochem.* **1970**, *36*, 222. (c) Wantanabe, T.; Honda, K. *J. Phys. Chem.* **1982**, *86*, 2617.

(22) Frei, H.; Fitzmaurice, D.; Grätzel, M. *Langmuir* **1990**, *6*, 198.

(23) Cusack, L.; Marguerettaz, X.; Rao, S. N.; Fitzmaurice, D., manuscript in preparation. The detailed reasons for the slower rate of decay of the transient assigned to long-lived trapped electrons in TiO<sub>2</sub>-(**CTAB+III**) as compared with TiO<sub>2</sub>-(**I+IV**) will be discussed here and supported by detailed NMR studies.

presence of longer-lived electrons trapped in the TiO<sub>2</sub> nanocrystallites of TiO<sub>2</sub>-I.<sup>19,20</sup> Consistent with the above and as opposed to aerated TiO<sub>2</sub>-(I and IV), a spectrum is measured for aerated TiO<sub>2</sub>-(CTAB and III) and is observed to agree well with that reported for photogenerated long-lived electrons trapped in TiO<sub>2</sub> nanocrystallites.<sup>19,20</sup> Second, on the basis of the difference of the final amplitudes of the millisecond transients (0.0005 au), an irradiation volume of 0.4 cm<sup>3</sup>, and a sample volume of 1.4 cm<sup>3</sup> one predicts a steady-state absorption of 0.02 au at 600 nm for degassed TiO<sub>2</sub>-(CTAB and III) by reduced III. On this basis, the microsecond transient in Figure 7b is assigned to electrons trapped in a TiO<sub>2</sub> nanocrystallite and to the radical cation of III or formed by diffusion to TiO<sub>2</sub>-CTAB. Finally, as there is no measurable absorption by the molecular components CTAB or III at 355 nm, no transients are measured for CTAB, III, or (CTAB and IV).

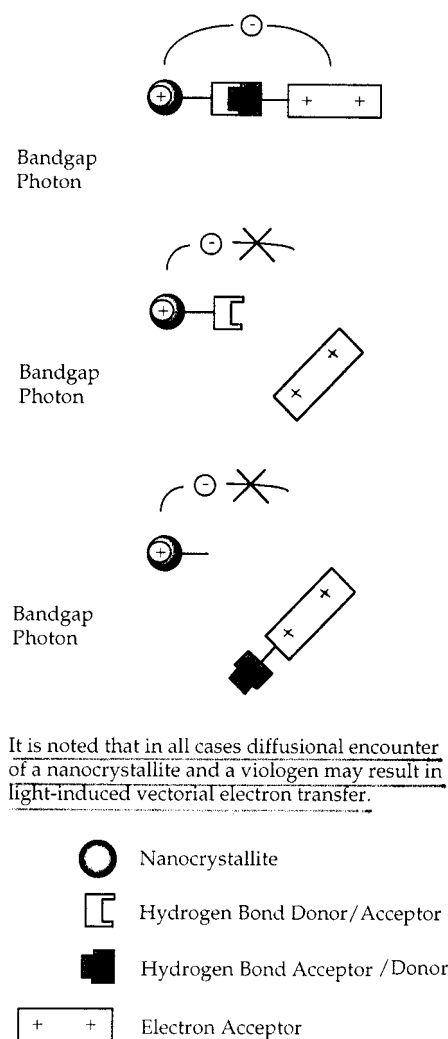
As the optical absorption at 355 nm of the nanocrystallite in TiO<sub>2</sub>-I nm is 0.1 au, the pulse energy is 2 mJ, the cross-sectional area for irradiation is 0.4 cm<sup>2</sup>, and assumed reflection losses are 20%, it is estimated that an average of 14 electron-hole pairs are generated per TiO<sub>2</sub> nanocrystallite. From the initial amplitude of the microsecond transient in Figure 6b for degassed TiO<sub>2</sub>-(I+III) and the known extinction coefficient for the reduced form of viologen,<sup>21</sup> it is estimated that one radical cation of III is formed on every third nanocrystallite. That is, the charge-separation efficiency is about 6% with the majority of the photogenerated electron-hole pairs being lost by recombination or trapping.<sup>19,20</sup>

The initial amplitudes of the microsecond transients for degassed TiO<sub>2</sub>-(I and IV) and TiO<sub>2</sub>-(CTAB and III) agree, within the experimental error of 2 × 10<sup>-4</sup> au, with the initial amplitude of the microsecond transient for degassed TiO<sub>2</sub>-I. On this basis, it may be concluded that no radical cations of IV and III respectively are formed within the laser pulse but are formed only on the millisecond time scale by diffusional encounter with TiO<sub>2</sub>-I and TiO<sub>2</sub>-CTAB, respectively. The possibility however, that radical cations of I and III are formed within the laser pulse cannot be completely excluded as it might reasonably be expected that the above species are initially sufficiently close to TiO<sub>2</sub>-I and TiO<sub>2</sub>-CTAB to be reduced.

It is noted that the molecular components of TiO<sub>2</sub>-(I+III), TiO<sub>2</sub>-(I and IV), or TiO<sub>2</sub>-(CTAB and III) may undergo oxidative degradation under prolonged irradiation in the absence of a suitable hole scavenger.<sup>24</sup> However, no evolution of the transients in Figures 6 or 7 that might be attributed to oxidative photodegradation of the molecular components was observed.

**IV. Concluding Comments.** TiO<sub>2</sub>-I containing a diaminopyridine moiety recognizes and selectively binds the modified viologen III containing a uracil moiety. Immediate light-induced vectorial electron transfer is observed for the resulting donor-acceptor complex. It is noted there is ample precedent for electron transfer over long distances in supermolecules and their organized assemblies.<sup>25</sup> In the absence of a uracil moiety the modified nanocrystallite TiO<sub>2</sub>-I does not recognize

Scheme 4



or selectively bind the viologen IV. Similarly, in the absence of a diaminopyridine moiety the modified nanocrystallite TiO<sub>2</sub>-CTAB does not recognize or selectively bind the modified viologen III. In neither case is immediate light-induced vectorial electron transfer to the viologen moiety observed. As expected, in all cases electron transfer is observed following diffusional encounter of the donor and acceptor in solution. These findings are summarized in Scheme 4.

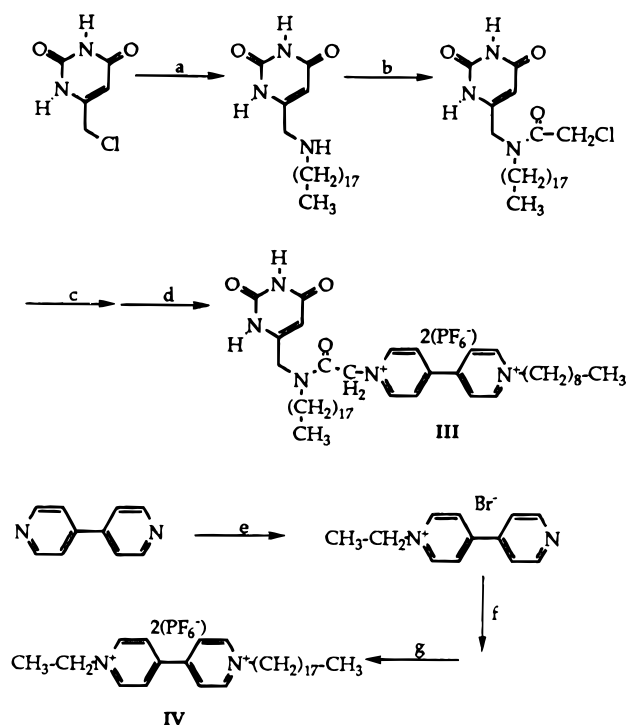
Generally, it is possible to modify a nanocrystallite so that it selectively binds a molecular substrate in solution. Further development of this and related chemistry is foreseen. For example, current studies are directed toward modifying the surface of a TiO<sub>2</sub> nanocrystallite to selectively bind other nanocrystallites in solution.<sup>26</sup> In this context we note recent closely related reports.<sup>27</sup> Looking further to the future, analogous approaches involving many condensed phase and mo-

(24) For example ethanol has been shown to act as an efficient hole scavenger in a number of studies: *Semiconductor Electrodes*, Finklea, H., Ed.; Elsevier: New York, 1988; p 113.

(25) (a) Sessler, J.; Wang, B.; Harriman, A. *J. Am. Chem. Soc.* **1995**, *117*, 704 and references therein. (b) Chidsey, C. *Science* **1991**, *251*, 919. (c) Finklea, H.; Hanshew, D. *J. Am. Chem. Soc.* **1992**, *114*, 3173. (d) Cleland, G.; Horrocks, B.; Houlton, A. *J. Chem. Soc., Faraday Trans.* **1995**, *91*, 4001.

(26) Cusack, L.; Fitzmaurice, D., manuscript in preparation.

(27) (a) Murray, C.; Kagan, C.; Bawendi, M. *Science* **1996**, *270*, 1335. (b) Mirkin, B.; Letsinger, R.; Mucic, R.; Storhoff, J. *Nature* **1996**, *382*, 607. (c) Alivisatos, P.; Johnson, K.; Xiaogang Peng; Wilson, T.; Loweth, C.; Bruchez, M.; Schultz, P. *Nature* **1996**, *382*, 609. (d) Kamat, P.; Bedja, I.; Vonodgopal, K. *Fine Particle Science and Technology*; Nato ASI Ser. 3, **1996**, *12*, 303.

**Scheme 5. Reaction Conditions for Synthesis of III and IV<sup>a</sup>**


<sup>a</sup> Octadecylamine, *i*-PrOH, reflux, N<sub>2</sub>; (b) chloroacetic anhydride, pyridine–chloroform, room temperature; (c) 4-nonylbipyridinium bromide, acetonitrile, reflux; (d) methanolic ammonium hexafluorophosphate; (e) excess ethyl bromide (neat), room temperature; (f) octadecyl bromide, acetonitrile, reflux; (g) as in (d).

molecular components may prove possible and offer the prospect of self-assembling complex heterosupramolecular structures. As discussed in detail elsewhere, such structures might be expected to form the basis of practical molecular scale devices.<sup>5</sup>

**Experimental Section**

**Synthesis of Condensed-Phase Components.** TiO<sub>2</sub> nanocrystallites were prepared, following the method of Kotov et al.,<sup>15</sup> by arrested hydrolysis of titanium tetraisopropoxide. Briefly, titanium tetraisopropoxide (12.5 μL in 2 mL of dry chloroform or chloroform-*d*) was added to 8 mL of chloroform or chloroform-*d* containing added water (2 μL). This addition was made under nitrogen during 3 h in the presence of added **I** (20 mg) or CTAB (15 mg) stabilizers.

**Synthesis of Molecular Components.** Molecular components **I** and **II** were prepared following methods previously reported by Lehn and co-workers.<sup>9</sup> Subsequent characterization was by elemental analysis and <sup>1</sup>H NMR.

Calculated for *N,N*-2,6-pyridinediylbis[undecamide] (C<sub>29</sub>H<sub>51</sub>N<sub>3</sub>O<sub>2</sub>, **I**): C, 73.53; H, 10.85; N, 8.87. Found: C, 73.60; H, 10.64; N, 8.91. <sup>1</sup>H NMR (chloroform-*d*) δ 0.88 (t, 6H, *J* = 7.0 Hz); 1.25–1.74 (m, 36H); 2.36 (t, 4H, *J* = 7.6 Hz); 7.52 (s, 2H, –NH amidic); 7.69 (t, 1H, *J* = 8.2 Hz); 7.88 (d, 2H, *J* = 8.2 Hz).

Calculated for 6-(*N*-tridecylundecamido)methyluracil (C<sub>30</sub>H<sub>55</sub>N<sub>3</sub>O<sub>3</sub>, **II**): C, 71.25; H, 10.95; N, 8.30. Found: C, 71.25; H, 10.95; N, 8.95. <sup>1</sup>H NMR (chloroform-*d*) δ 0.88 (t, 6H, *J* = 7.0 Hz); 1.26–1.58 (m, 40H); 2.36 (t, 2H, *J* = 7.8 Hz); 4.16 (s, 2H); 5.52 (s, 1H); 8.14 (s, 1H, –NH amidic); 9.51 (s, 1H, –NH imidic).

The molecular components **III** and **IV** were synthesized as shown in Scheme 5 and also characterized by elemental analysis and <sup>1</sup>H NMR.

Calculated for 4-nonyl-4'-[*N*-octadecyl-*N*-(6-uracilmethyl)aminocarbonyl methyl]bipyridinium bis(hexafluorophosphate) (C<sub>44</sub>H<sub>71</sub>N<sub>5</sub>O<sub>3</sub>P<sub>2</sub>F<sub>12</sub>, **III**): C, 52.42; H, 7.10; N, 6.95. Found: C, 52.02; H, 7.02; N, 6.83. <sup>1</sup>H NMR (acetone-*d*<sub>6</sub>) δ 0.86 (t, 6H, *J*

= 6.7 Hz); 1.28–1.39 (m, 46H); 3.60 (t, 2H, *J* = 7.8 Hz); 4.52 (s, 2H); 5.00 (t, 2H, *J* = 7.6 Hz); 5.52 (s, 1H); 6.32 (s, 2H); 7.5 (br s, 1H, –NH amidic); 8.87–8.91 (dd, 4H, *J* = 5.1, 2.0 Hz); 9.35 (d, 2H, *J* = 7.3 Hz); 9.49 (d, 2H, *J* = 7.1 Hz); 9.90 (s, 1H, –NH imidic).

Calculated for 1-ethyl-1'-octadecyl-4,4'-bipyridinium bis(hexafluorophosphate) (C<sub>30</sub>H<sub>50</sub>N<sub>2</sub>P<sub>2</sub>F<sub>12</sub>, **IV**): C, 49.44; H, 6.92; N, 3.85. Found: C, 50.00; H, 7.11; N, 3.84. <sup>1</sup>H NMR (acetone-*d*<sub>6</sub>) δ 0.88 (t, 3H, *J* = 6.6 Hz); 1.28–1.32 (m, 32H); 1.80 (t, 3H, *J* = 7.4 Hz); 4.96 (q, 4H, *J* = 7.4 Hz); 8.85 (dd, 4H, unresolved coupling); 9.43 (d, 2H, unresolved coupling); 9.46 (d, 2H, unresolved coupling).

Cetyltrimethylammonium bromide (CTAB) was used as supplied without further purification. The results of the characterization of this compound by <sup>1</sup>H NMR are given for comparison. <sup>1</sup>H NMR (chloroform-*d*) δ 0.88 (t, 3H, *J* = 6.6 Hz); 1.25–1.36 (m, 28H); 1.78 (m, 2H); 3.50 (s, 9H).

**Self-Assembly of Supermolecules and Heterosupermolecules.** A solution (8 × 10<sup>-3</sup> mol dm<sup>-3</sup>) of the required molecular component was prepared in chloroform or chloroform-*d* (**II**) or acetone or acetone-*d*<sub>6</sub> (**III** and **IV**) and added to an equal volume of TiO<sub>2</sub>-**I** or TiO<sub>2</sub>-CTAB in chloroform or chloroform-*d* following a 2-fold concentration of the latter by evaporation. The final concentration of TiO<sub>2</sub> nanocrystallites was 4 × 10<sup>-7</sup> mol dm<sup>-3</sup>. The final concentration of **I**, **II**, **III**, **IV**, and CTAB was 4 × 10<sup>-3</sup> mol dm<sup>-3</sup>. In the case of transient absorption experiments the concentration of molecular components used was 10 times lower, i.e., 4 × 10<sup>-4</sup> mol dm<sup>-3</sup>.

**Characterization Techniques.** <sup>1</sup>H NMR spectra were recorded using either a JEOL JNM-GX270 FT or Varian 500 FT spectrometer at 20 °C unless otherwise stated. IR spectra were recorded using a Mattson Galaxy 3000 FT spectrometer (CaF<sub>2</sub> windows, 0.20 mm path length) at 20 °C unless otherwise stated. Optical absorption spectra were recorded using a Hewlett-Packard 8452A diode array spectrophotometer at 20 °C unless otherwise stated. Transmission electron micrographs were recorded using a JEOL 2000 FX TEMSCAN.

**Real-Time Transient Optical Absorption Spectroscopy.** Real-time transient optical absorption measurements were made using a spectrometer based on a previously described design.<sup>28</sup> Briefly, the continuous output of a Coherent argon ion laser (Innova 70-5) was used to pump a Coherent dye laser (Model 599-01 with rhodamine 6G). The dye laser output at 600 nm (ca. 200 mW cm<sup>-2</sup>) was split (40/60%) into two beams. One beam (40%) was allowed fall directly incident on one photodiode of a dual-diode detector. The second beam (60%) passed through the sample before falling incident on the second photodiode of the detector. The detectors used were United Detector Technology PIN-10D silicon photodiodes protected against scattered 355 and 532 nm light by a Melles Griot OG-550 optical cuton filter. The associated circuitry was configured to generate a dc voltage proportional to the difference in intensity of the two beams incident on the dual-diode detector. This signal was amplified and digitized using a Le Croy 9410 oscilloscope. The sample was excited at right angles to the probe beam using the pulsed output (single-shot or 10 Hz) of a Continuum-Surlite Nd:YAG laser. The above transient absorption spectrometer is capable of measuring absorption changes of 5 × 10<sup>-5</sup> absorbance units.

All absorption transients were recorded, unless otherwise stated, at 600 nm following pulsed excitation at 355 nm (5 ns, 2 mJ pulse<sup>-1</sup>) of rigorously degassed samples contained in a vacuum tight 1 cm by 1 cm quartz cell. Transients reported on the microsecond time scale are the average of 10 measurements, those reported on the millisecond time scale are the average of 100 measurements.

**Acknowledgment.** This work was supported by a grant from the Commission of the European Union (Contract JOR3-CT96-0107) and Forbairt (Contract SC-95-203).

CM9605173